Model of a Microfluidic Thermal Cycler Activated by Means of Electro-Osmotic Micro-Pumps

Elena Bianchi[1,2*], Maria Francesca Bello[1], Ida Critelli[1], Gabriele Dubini[1]
*Corresponding author: elena3.bianchi@mail.polimi.it

(1) Politecnico di Milano, LaBS, Laboratory of Biological Structure Mechanics, Milano, Italy
(2) Swiss Federal Institute of Technology (EPFL), Laboratory of Life Sciences Electronics - Swiss Up Chair, Lausanne, Switzerland

Abstract:
A microfluidic thermal cycler for Polymerase Chain Reaction (PCR) has been modeled. A microliter sample is driven along the microchannel by a flow generated by means of electroosmotic micropumps, activated in sequence. Several multichannel pumps configurations have been separately modeled and the efficiency of each device has been evaluated with regard to the effective flowrate and the back flowrate.
Results from these simulations have been then used to define the boundaries for the model of the entire device.

Keywords: microfluidics, electroosmosis, micropump, polymerase chain reaction, thermal cycler.

1. Introduction

A microfluidic thermal cycler activated by electroosmotic micro-pumps has been modeled (Fig.1). The main intended application of such a device is Polymerase Chain Reaction (PCR), a well-known procedure in molecular biology able to amplify and simultaneously quantify a targeted DNA molecule. Sample has to be thermal cycled along three main temperature steps (368, 328 and 345 K), enabling the denaturation of the strands, the annealing of the "primer" and the elongation of the new strand. Electroosmosis (EO) is an electrokinetic phenomenon. When a polar fluid and a solid surface are brought into contact, the superficial charge, characterized by the zeta potential ζ [mV], induces the formation of a double-charged layer. The presence of an external electric field forces this layer to move, dragging the fluid in the channel and resulting in a flat velocity profile. Electroosmotic pumps are then advantageous in microfluidic because of their compactness and the absence of moving parts [1,2,3,4].

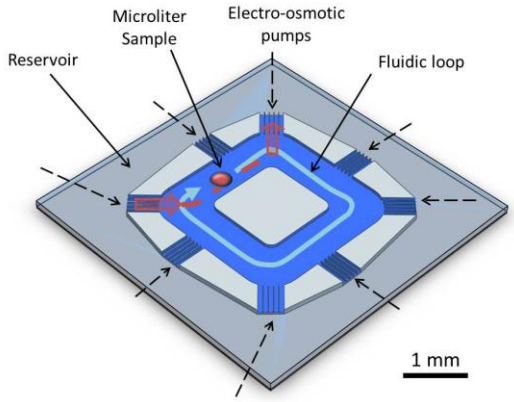

Figure 1: Microfluidic thermal cycler that consists of a fluidic loop in which the flow is generated by electroosmotic micropumps placed around the fluidic loop, activated in sequence.

2. Materials and Methods

The parallel channel configuration has been selected for the design of electroosmotic pumps. A set of pumps has been placed around a channel loop, connected to an external reservoir. The sample in the form of a drop, is brought along the channel, flowing through three different temperatures. 3D model of different pump configurations have been set (Fig.2). An electroosmotic velocity V_{EOF} has been defined at each wall. V_{EOF} is a function of the electric field $E_{EL,}$ generated by the potential V_0 and V_1 = 10 V, imposed at the heads of the channels. The flowrate Q_{EFF} delivered by each configuration has been evaluated in different temperature settings.
An EO pump configuration has been selected on the basis of the previous simulations.

Based on the results of these simulations flowrate boundary conditions for the entire devices have been defined (Fig.3 – blue solid lines). Time to cycle of the sample in the channel has been computed.

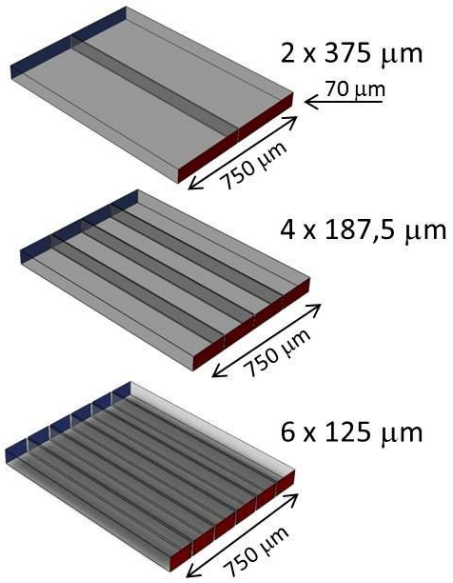

Figure 2: Pump configurations considered for 3D models.

3. Use of COMSOL Multiphysics

To simulate the performance of a multichannel EO pump an electroosmotic velocity V_{EOF} has been imposed at each wall, following the Helmotz-Smoluchowski equation (Eq.1):

$$V_{EOF} = \frac{\zeta \cdot \varepsilon \cdot E_{EL}}{\mu} \qquad \text{(Eq.1)}$$

with E_{EL} the electric field, ε [-] the permittivity, µ [Pa ·s] the fluid viscosity, ζ [mV] the Zeta Potential. ζ and µ are considered as functions of the temperature. To the heads of the channels voltage, temperature and pressure conditions have been imposed: $V_1 = 10$ V, $P_0 = 0$ Pa and T = 293,15 K at the inlet; $V_0 = 0$ V, T = 345/328/368 K, $P_1 = r_C \cdot Q$ Pa at the outlet, where Q is the flow-rate [mm^3/s] and r_C the value of the hydraulic resistance faced by the pump if connected to the loop [5]. The flowrate Q_{EFF} delivered by each configuration has been evaluated.

In the simulation of the entire fluidic loop the pumps have been simulated by flowrate inlet and outlet functions (Fig.3). Q_{IN} and Q_{OUT} are sums of the electroosmotic flowrate Q_{EOF} (in the case of $\Delta P = 0$) and the back-flowrate Q_{BFLOW}, induced by the downstream hydraulic resistance. Q_{EOF} is an inlet flowrate in the case of Q_{IN}, while it is an outgoing flowrate in the case of Q_{OUT},.

The time-dependent simulation of the flow in the fluidic loop, generated by EO pump activated in sequence is a 2D model with the shallow channel approximation. It considers the effect of planar channel walls (thickness h = 70 µm) by means of a volume forces term F_W (Eq.2), with

$$F_W = -\frac{12 \cdot \mu \cdot \vec{u}}{h^2} \qquad \text{(Eq.2)}$$

µ [Pa·s] the dynamic viscosity, $\vec{u}$ [m/s] the velocity and *h* [m] the channel thickness.

A proper sequence of pumps activation, couple by couple, has then been implemented in a time - dependent simulation.

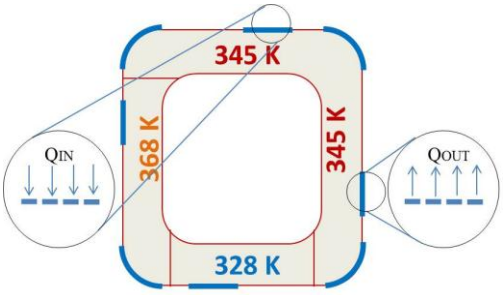

Figure 3: Fluidic loop with dimensions and temperature zones. Pumps are activated couple by couple, by defining one pump as a Q_{IN} function and the other as a Q_{OUT}.

4. Results

A number of pump configurations have been evaluated to identify the pumping device to be integrated around the microfluidic fluidic loop. Number of channels *n* and different conditions of temperature T (zeta potential ζ is a function of T) have been considered to evaluate efficiency of

the pump configuration on a fixed pumping section of h = 70 μm and w = 750 μm.
The velocity field has been evaluated considering the presence of three different temperature zones along the fluidic loop, higher than the environment temperature (293,15 K).
In Fig.4 it can be seen that V_{EOF} increases with the temperature, depending on the trend of potential ζ. When the outlet temperature is higher than the inlet one, V_{EOF} is greater around the outlet: the velocity in the middle of the channel section decreases with the temperature, according to the conservation law of the mass.

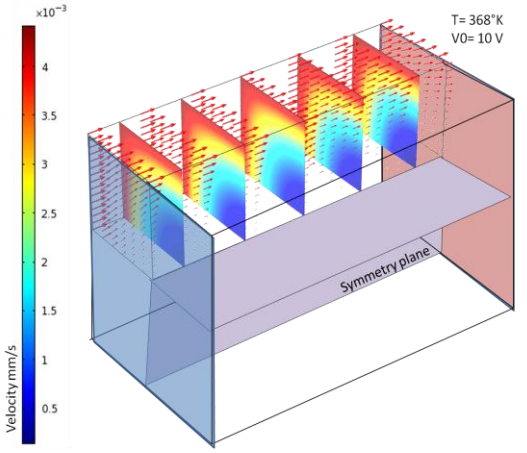

Figure 4: Velocity profile in a EO microchannel with a temperature difference of 293 to 368 K from inlet to outlet.

Pumps have been evaluated in three temperature scenarios, corresponding to the working temperatures of this PCR device.
As shown in Fig.5, Q_{EFF} is a function of the number of parallel channels *n* (2 - 4 - 6 channels). Q_{EFF} increases with the number of channels of the pump. The highest Q_{EFF} corresponds to the highest difference in temperature between the heads of the channel. The configuration of pump suitable for the device is then the *n* = 6, which shows the highest Q_{EFF} in all the temperature scenarios.

In the 2D time-dependent model of the fluidic loop the pumps are described by Q_{IN} and Q_{OUT} functions associated to each single channel composing the six-channel pump. Q_{IN} and Q_{OUT} are implemented as shown in Eq.3a and Eq.3b. P_d is the average pressure at the boundary and r_{CB} is the hydraulic resistance that stands for the single pumping channel.

$$Q_{IN} = Q_{EOF} - \frac{P_d}{r_{CB}} \qquad \text{(Eq.3a)}$$

$$Q_{OUT} = -Q_{EOF} - \frac{P_d}{r_{CB}} \qquad \text{(Eq.3b)}$$

The trend of the Q_{EOF} related to the single channel is shown in Fig.6 as a function of the width w.

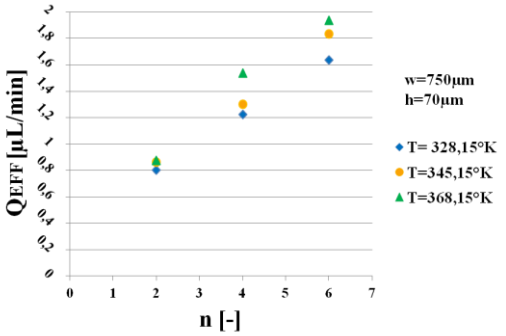

Figure 5: Q_{EFF} values for each pump configurations as functions of the number of pumping channels *n*, for the three different temperature scenarios.

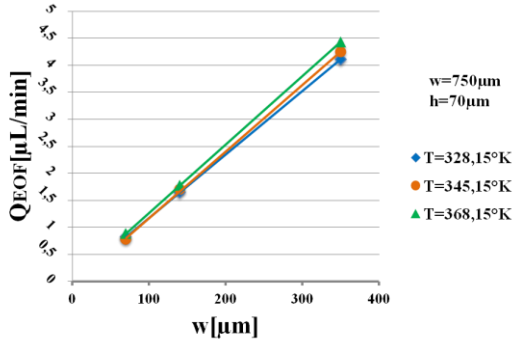

Figure 6: Q_{EOF} trend of a single channel as a function of the width w, for the three different scenarios. In the six-channel selected configurations w = 125 μm.

The six-channel configuration has been selected and implemented into the model of the fluidic loop (Fig.7).
The activation timing of each couple of pumps is generated by rectangular functions (Fig.8) with a proper activation and de-activation smoothing interval to avoid discontinuity points, which also

helps the convergence of the simulation. It is showed that the highest value of Q_{IN} supplied by the inlet pump is 1,8 µL/min and that the related time to cycle is ~50 s.

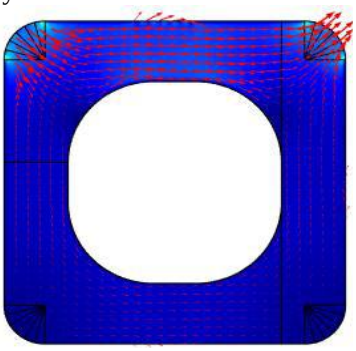

Figure 7: Velocity color map of flow in the channel from the 2D time dependent simulation. Velocity vectors show the activated pumps.

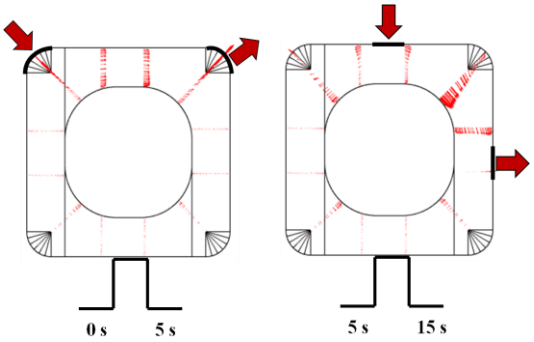

Figure 8: Activation timing for two consecutive couples of pumps. Vectors represent the velocity of flow on selected channel sections (not to scale).

5. Conclusions

Results of the simulations show a consistent performance of the micro-thermo-cycler in term of continuity in time and directionality. Priming volumes and times to cycle are compatible to the usual parameters characterizing a PCR protocol.
This kind of configuration allows to avoid the direct immersion of a biological sample in the electric field.
Furthermore this kind of device allows the sample cycle without using external pumps.

8. References

1.Wang, X., et al., Electroosmotic pumps and their applications in microfluidic systems. Microfluidics and Nanofluidics, 2009. 6(2): p. 145-162.

2. Brask, A., G. Goranović, and H. Bruus, Theoretical analysis of the low-voltage cascade electro-osmotic pump. Sensors and Actuators, B: Chemical, 2003. 92(1-2): p. 127-132.

3.Y.Berrouche,Y.Avenas,C.Schaeffer,H.C.Chang, P.Wang, “Design of a porous electroosmotic pump used in power electronic cooling”, IEEE transactions on industry applications, VOL.45, NO.6, 2009

4. Q.Guo, Y.Liu, X.Wu, J.Yang, “Design of a relaying electroosmosis pump driven by low-voltage DC”, Microsystem Technology (2009) 15: 1009-1015

5. Z.Wu, K.Hjort, “Microfluidic Hydrodynamic Cell Separation: A Review”, Micro and Nanosystems, 2009.